

# COMPUTATIONAL FLUID DYNAMICS (CFD) INVESTIGATION TO ASSESS WIND EFFECTS ON A TALL STRUCTURES (WIND FORCE PARAMETERS)

G Naga Sulochana<sup>1</sup>, H Sarath kumar<sup>2</sup>

<sup>1</sup>M.Tech Student. <sup>2</sup>Assistant Professor

<sup>1,2</sup>Department of Civil Engineering, AVR & SVR College of Engineering and Technology, Nandyal.

\*\*\*

**Abstract** - The development of high strength concrete, higher grade steel, new construction techniques and advanced computational technique has resulted in the emergence of a new generation of tall structures that are flexible, low in damping, slender and light in weight. These types of flexible structures are very sensitive to dynamic wind loads and adversely affect the serviceability and occupant comfort. This project presents the results using Computational Fluid Dynamics Technique using Gambit & Fluent software on square building models with an acceptance ratio of 1:1.5:7. The wind force on the models is evaluated from force records obtained from software under Computational Fluid Dynamics Technique using Gambit & Fluent for normal wind directions in a sub-urban terrain conditions for category A. The same rectangle building analyzed manually by IS 875 Part 3: 1987. The value obtained from this are compared with software results. The further study is made for the design and calculation of Gust Response Factor.

**Keywords** : Windward, Leeward, Guest Response, Acceptance Ratio.

## 1.INTRODUCTION

### Importance Of wind Analysis on Tall Structures:

Wind is air in motion relative to the surface of the earth. The primary cause of wind is traced to earth's rotation and differences in terrestrial radiation. The radiation effects are primarily responsible for convection either upwards or downwards. The wind generally blows horizontal to the ground at high wind speeds. Since vertical components of atmospheric motion are relatively small, the term 'wind' denotes almost exclusively the horizontal wind, vertical winds are always identified as such. The wind speeds are assessed with the aid of anemometers or anemographs which are installed at meteorological observatories at heights generally varying from 10 to 30 meters above ground.

Very strong winds (greater than 80 km/h ) are generally associated with cyclonic storms, thunderstorms, dust storms or vigorous monsoons. A feature of the. Cyclonic storms over

the Indian area is that they rapidly weaken after crossing the coasts and move as depressions/lows in land. The influence of a severe storm after striking the coast does not, in general exceed about 60 kilometers, though sometimes, it may extend even up to 120 kilometers. Very short duration hurricanes of very high wind speeds called KalBaisaki or Norwesters occur fairly frequently during summer months over east India.

The liability of a building to high wind pressures depends not only upon the geographical location and proximity of other obstructions to air flow but also upon the characteristics of the structure itself

The effect of wind on the structure as a whole is determined by the combined action of external and internal pressures acting upon it. In all cases, the calculated wind loads act normal to the surface to which they apply.

The stability calculations as a whole shall be done considering the combined effect, as well as separate effects of imposed loads and wind loads on vertical surfaces, roofs and other part of the building above general roof level. Buildings shall also be designed with due attention to the effects of wind on the comfort of people inside and outside the building.

## 2.LITERATURE SURVEY

### 2.1 Wind Characteristics:

#### Basic Wind Pressures:

Figure 1 gives basic wind speed map of India, as applicable to 10 m height above mean ground level for different zones of the country. Basic wind speed is based on peak gust velocity averaged over a short time interval of about 3 seconds and corresponds to mean heights above ground level in an open terrain (Category 2 ). Basic wind speeds presented in Fig. 1 have been worked out for a 50 year return period. Basic wind speed for some important cities/towns

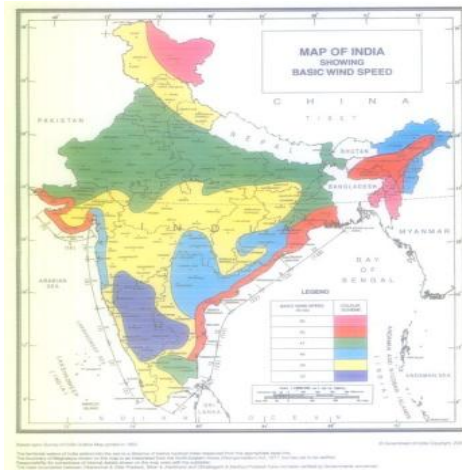


**Fig. 1 Basic Wind Speed**

**2.2 Gradient Wind Speed:**

The gradient wind is a balance of the Pressure Gradient Force, centrifugal and Coriolis. A geotropic wind becomes a gradient wind when the wind begins flowing through curved height contours. The curving motion introduces a centrifugal (outward fleeing) force. The centrifugal effect can be felt when turning through a curve in a car. You stay with the car but it feels like you are being pushed sideways.

**2.3 Gust Factor:**

Only the method of calculating load along wind or drag load by using gust factor method is given in the code since methods for calculating load across-wind or other components are not fully matured for all types of structures. However, it is permissible for a designer to use gust factor method to calculate all components of load on a structure using any available theory. However, such a theory must take into account the random nature of atmospheric wind speed.

**2.4 Turbulence characteristics**

Gustiness occurs due to the velocity fluctuations present in the wind flow and this renders the forces exerted on the structure as dynamic forces. The degree of gustiness is given by standard deviation or RMS velocity value. The turbulent intensity can be obtained from SD and mean velocity and is given in equation.

$$I_u = \left( \frac{\sigma_u}{\bar{U}} \right) \text{ or } I_u = \left( \frac{1}{\ln(z/Z_0)} \right)$$

where

$I_u$  = turbulent intensity

$\sigma_u$  = standard deviation

$\bar{U}_z$  = mean velocity at height 'z'

$Z_0$  = terrain roughness length

Wind velocity has two components which are mean velocity that increases with height and turbulent velocity that remains same after gradient height. The variation of wind velocity with time has been illustrated in Fig. 3.3 and is given in equation

$$V_t = V + V'$$

Where,

$V_t$  = wind velocity at any given instant of time 't'

$V$  = average wind

$V'$  = wind gusts

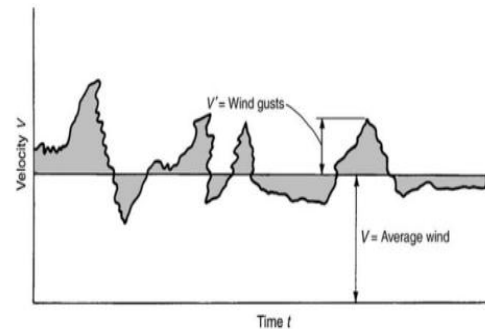


**Fig. 2 Variation of wind velocity with time**

As wind pressures are proportional to the square of velocities, with variation of mean Wind velocity, the mean pressures also fluctuate. The variation of pressure has been shown in Fig.2 and is given by:

$$P_t = P + P'$$

Where,

$P_t$  = pressure at any instant of time 't'

$P$  = Mean pressure

$P'$  = Gust pressure

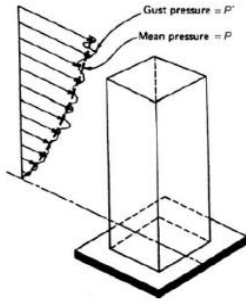


**Fig 3. Schematic representation of mean and gust pressure at any instant of time 't' Along wind and across wind motions**

Under the action of wind flow, structure experience aerodynamic forces that include the drag force and lift force. Drag (along-wind) force acting in the direction of the mean wind and the lift (across-wind) force acting perpendicular to that direction. The Along-wind motion primarily results from pressure fluctuations in the windward and the leeward faces, which generally follow the fluctuations in the approach flow. The Across-wind motion is introduced by pressure fluctuations due to vortex shedding in the separated shear layers and wake flow field.

**2.5 Wind force F**

**Along Wind Load** - Along wind load on a structure on a strip area (  $A_e$  ) at any height (Z) is given by:

$$F_s = C_f A_e P_z G$$

where

$F_s$  = along wind load on the structure at any height z corresponding to strip area  $A_e$

$C_f$  = force coefficient for the building,

$A_e$  = effective frontal area considered for the structure at height Z,

$P_z$  = design pressure at height z due to hourly mean wind obtained as  $0.6 V_z^2$  (N/m<sup>2</sup>)

**3. Data Collection**

**Evaluation of wind force**

Fig.10 (IS 875-3 Pg.51) shows the different faces of angles considered for the pressure measurement study. The chord length for each face is given as follows: Face A: 0- 10cm, Face B: 10- 25cm, Face C: 25- 35cm, Face D: 35- 50cm

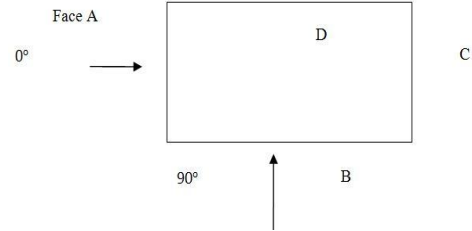


**Fig. 4 Forces acting on building**

LEVELS	Z/H	HEIGHT in cm	Fx1987(0°)	Fy1987(90°)
1.000	0.1	7	904	448
2.000	0.2	14	1224	596
3.000	0.3	21	1421	686
4.000	0.5	35	3474	1673
5.000	0.7	49	3874	1859
6.000	0.8	56	2052	984
7.000	0.9	63	2257	1063
8.000	0.95	66.5	1197	586
9.000	1	70	1310	623
1.000	0.1	7	904	448

**Table 7 Calculation of force as per IS-875(part-3) 1987 Provisions**

Level	Leeward (90°)	Windward(0°)
1.000	447.813	904.415
2.000	596.178	1224.411
3.000	686.036	1420.865
4.000	1673.259	3473.529
5.000	1859.123	3874.313
6.000	983.512	2052.260
7.000	1062.681	2256.651
8.000	585.652	1196.696
9.000	622.840	1310.187

**Table 7 Calculation of force as per IS-875(part-3) 1987 Provisions**

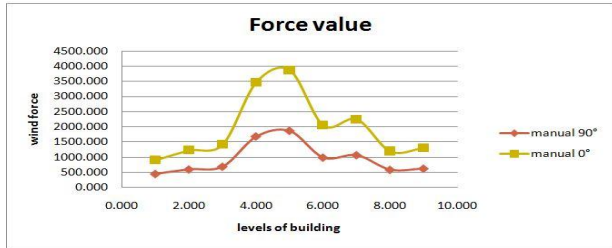


**Fig. 5 Forces for manual solutions**

**4. RESULTS AND DISCUSSION**

Unsteady numerical simulations have been carried out for a 1:2:5 rectangular building model under uniform wind flow condition using two types of turbulence models available in FLUENT 6.3 software: (i) Realizable k-ε turbulence model, which is single scale type turbulence model and (ii) DES turbulence model with Realizable k-ε option, which is multi-scale type hybrid turbulence model. For the evaluation of pressure coefficients and drag and lift force coefficients, the reference wind velocity is taken as 10 m/s (same as the uniform input wind velocity) and reference area of projected area, i.e. 0.1 m x 0.5 m. Unsteady simulations have been carried out until stabilized mean and standard deviation values of Cd and Cl are obtained with respect to time as shown in Fig.9 in IS 875-3 Pg.50 for Realizable k-ε turbulence model.

A MATLAB program has been developed for processing the numerically simulated Cp values to obtain distributions of mean Cp and standard deviation Cp values at 5 selected levels, viz. 0.05 m, 0.15 m, 0.25 m, 0.35 m, 0.45 m,

respectively (correspond to z/H values of 0.1, 0.3, 0.5, 0.7, 0.9 ref. Level 1, Level 2, Level 3, Level 4, Level 5). Further mean Cd and standard deviation Cl values have been at these 5 levels and also for the overall building also. The following sections discuss some these results.

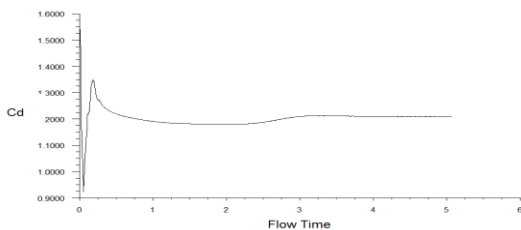


**Fig. 6: Variation of drag coefficient with time - Realizable k-ε turbulence model**

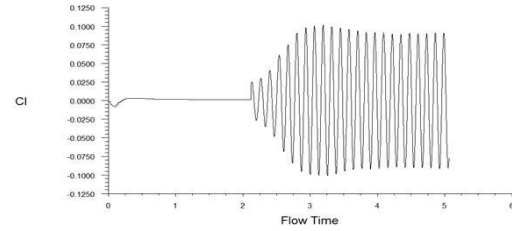


**Fig 7: Variation of lift coefficient with time - Realizable k-ε turbulence model**

**Velocity Vector Plots**

Figs. 6 and 7 show the velocity vector plot on center vertical plane for Realizable k-ε case. It can be seen over the roof of building significant increase in wind velocity due to separation from the windward edge of the roof. Further in the wake region, i.e. rear side of the building, flow with recirculation is observed with wind in opposite direction along with vertical wind near to building rear side Fig.10 in IS 875-3 Pg.51 shows the velocity vector plot for DES case. Unlike for Realizable k-ε case, it Can be seen multiple eddies in the wake region of the building, which is due to DES model can simulate multi-scale turbulence, i.e. eddies with different sizes.

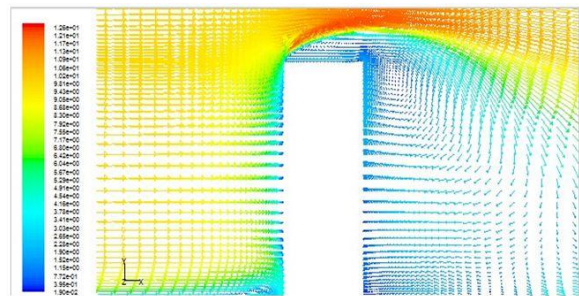


**Fig. 8: Velocity vector plot on center vertical plane - Realizable k-ε turbulence model**

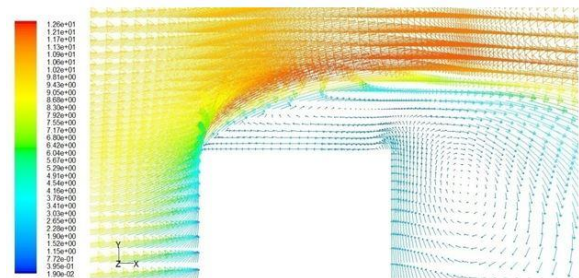


**Fig. 9 Close up view of velocity vector plot near building roof on center vertical plane- Realizable k-ε turbulence model**

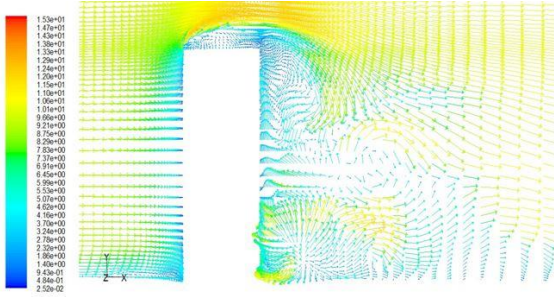


**Fig. 10 Velocity vector plot on center vertical plane - DES turbulence model**

**Vorticity Contours**

Vorticity is a measure of the rotation of a fluid element as it moves in the flow field and is defined as the curl of the velocity vector. It is show the vorticity contour plots in horizontal plane at Level 1, Level 3 and Level 5, respectively for Realizable k-ε turbulence model. It can be seen that the vortex shedding is predominant at Level 1 and as the height of the level increases, the vortex shedding phenomenon is observed to be affected. This is due to the wind flow from the top of the building into the wake region affecting the vortex shedding in the top region of the wake. Similarly Fig.9 in IS 875-3 Pg.50 show the vorticity contour plots in horizontal plane at Level 1, Level 3 and Level 5, respectively for DES turbulence model. Similar to Realizable k-ε predictions, the vortex shedding phenomenon is observed to be affected in the top region of the wake. However, DES predictions show vortex shedding with multiple eddies in the wake region.

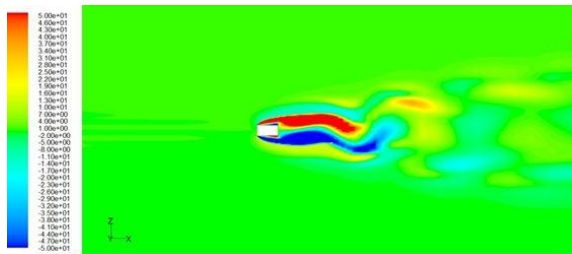


**Fig. 11 Vorticity Contour in horizontal plane at Level 1 - Realizable k-ε turbulence model**

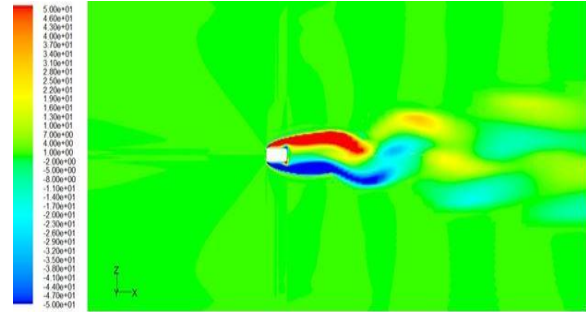


**Fig. 12 Vorticity Contour in horizontal plane at Level 3 - Realizable k-ε turbulence model**

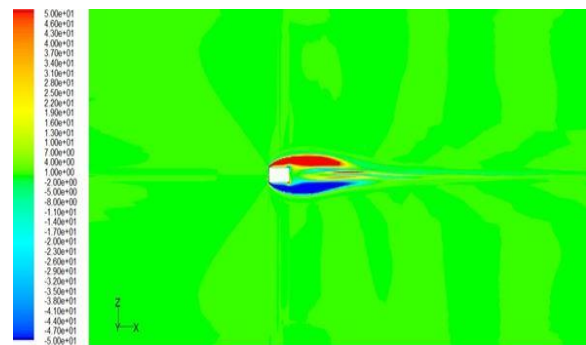


**Fig. 13 Vortices Contour in horizontal plane at Level 5 - Realizable k-ε turbulence model**

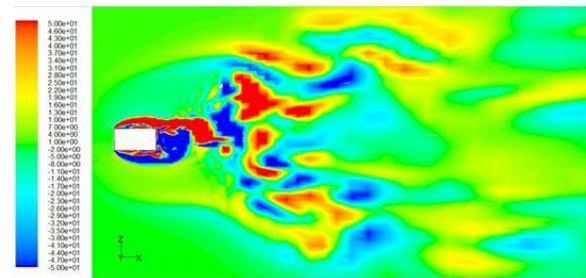


**Fig. 14 Vorticity Contour in horizontal plane at Level 1 - DES turbulence model**

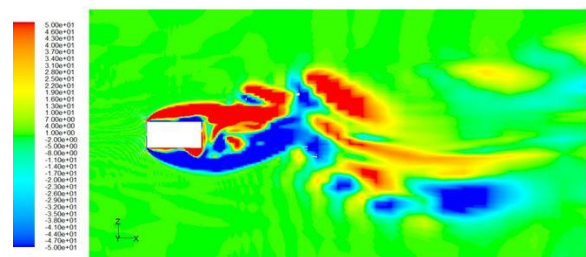


**Fig. 15 Vorticity Contour in horizontal plane at Level 3 - DES turbulence model**

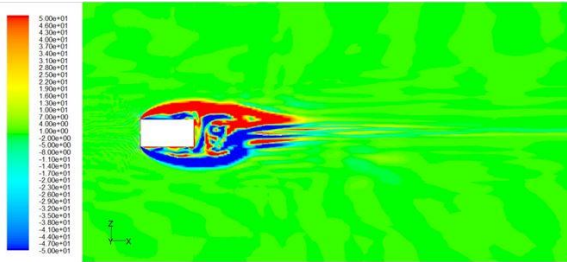


**Fig. 16 Vorticity Contour in horizontal plane at Level 5-DES turbulence model Mean Cp Distributions**

Fig.10 in IS 875-3 Pg.51 show the mean Cp contour on the rectangular building obtained using Realizable k-ε and DES turbulence models, respectively. It can be seen that on the front face, the mean Cp variation along the height is observed to be mostly uniform except at top and bottom regions, where the edge effects are expected. On the back face, the mean Cp values are observed to be negative, i.e

suction pressure and their magnitudes are observed to be increasing with increase in height. However, on the side faces, difference in the mean Cp distributions is observed between the two turbulence models.

Further, mean Cp distributions along the circumference of the building at 5 levels, viz. Level 1, 2, 3, 4 and 5, have been shown in Fig.10 in IS 875-3 Pg.51 based on the Realizable k-ε and DES turbulence models, respectively. It can be seen that for both the turbulence models, on the front face, the mean Cp values are almost same for Levels 2, 3 and 4, whereas at Levels 1 and 5, the mean Cp values are less. On the back face, in general, the mean Cp suction magnitudes are observed to be increasing with increase in height. On the side face, the mean Cp values are observed to be same for all the levels except for Level 1 in the case of Realizable k-ε turbulence model .

Fig.10 in IS 875-3 Pg.51 show the distribution of mean Cp along the circumference for levels 1, 3 and 5, respectively, to study the difference between the predictions of Realizable k-ε and DES turbulence models. It can be seen that on the front face both the turbulence models predict almost same mean Cp values. However, the mean Cp suction magnitudes on the side and back faces are observed to be more in the case of DES turbulence model than those in the case of Realizable k-ε turbulence model. At Level 1, Realizable k-ε turbulence model is observed to predict pressure recovery on the side faces from the windward edge. At Level 5, the mean Cp distribution along the side and back faces are observed to be nearly uniform based on both the turbulence models.

LEVELS	Z/H	HEIGHTS in cm	Fx 1987(0°)	Fy 1987(90°)
1.000	0.1	7	900	438
2.000	0.2	14	1200	586
3.000	0.3	21	1411	676
4.000	0.5	35	3464	1573
5.000	0.7	49	3864	1759
6.000	0.8	56	2042	974
7.000	0.9	63	2157	963
8.000	0.95	66.5	1297	566

**Table 7 Calculation of force as per IS-875(part-3) 1987 Provisions**

Level	Leeward (90°)	Windward(0°)
1.000	900	438
2.000	1200	586
3.000	1411	676
4.000	3464	1573
5.000	3864	1759
6.000	2042	974
7.000	2157	963
8.000	1297	566
9.000	622.840	1310.187

**Table 7 Calculation of force as per IS-875(part-3) 1987 Provisions**

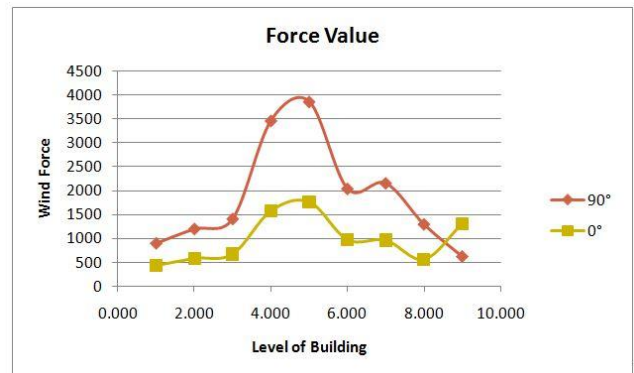


**Fig. 17: Forces for software solutions**

	manual 90°	manual 0°	software 90°	software 0°
1.000	447.813	904.415	900	438
2.000	596.178	1224.411	1200	586
3.000	686.036	1420.865	1411	676
4.000	1673.259	3473.529	3464	1573
5.000	1859.123	3874.313	3864	1759
6.000	983.512	2052.260	2042	974
7.000	1062.681	2256.651	2157	963
8.000	585.652	1196.696	1297	566
9.000	622.840	1310.187	632.840	310.187

**Table 7 Comparison of force for both manual and software solutions**



**Fig. 18 Comparison of force for both manual and software solutions**

**5. CONCLUSIONS**

Mean force value for 0° for Level 5 is always higher than all the other levels due to greater area of projection and edge effect at the ground level. For all other levels, values are almost same with draft code and IS: 875 (part-3) 1987 which indicates that these values are mostly governed by buffeting characteristics of approaching wind flow.

Mean force value for 0° for Level 5 is always higher than all the other levels due to greater area of projection and edge effect at the ground level. For all other levels, values are greater than with draft code and IS: 875 (part-3) 1987 of 0.2 ratio which indicates that these values are not governed by buffeting characteristics of approaching wind flow.

Standard deviation of force coefficients shows decrease in value with height which shows that these parameters depend on the decrease in turbulence intensity with height.

The mean value of drag and lift coefficients obtained from IS: 875 are 2.0547 and 1.9287 and Draft code value obtained 2.1994 and 2.1809 and experimental value obtained is 2.0374 and 1.7845, which is in good agreement with code values for 0° but for 90°, these values are differing this is due to Wake Effect.

The value of force obtained from IS 875 Part 3 447.813 for 90° it is the drag coefficient and 900 for 90° with Gambit and Fuent. This variation is due to vertex shedding at all levels.

**6. REFERENCES**

- Alexandre Luis Braun and Armando Miguel Awruch, 2009. Aerodynamic and aeroelastic analyses on the CAARC standard tall building model using numerical simulation. Computers and Structures, 87, 564–581
- Huang M.F., HLau I.W., Chan C.M., Kwok K.C.S. and G.Li, 2011. A hybrid RANS and kinematic simulation of wind load effects on full-scale tall buildings. Journal Wind Eng. Ind. Aerodyn, 99, 1126–1138.
- Shenghong Huang, Lib Q.S. and Shengli Xua, 2007. Numerical evaluation of wind effects on a tall steel building by CFD. Journal of Constructional Steel Research, 63, 612–627.
- Claudio Mannini, Ante Soda and Gunter Schewe, 2011. Numerical investigation on the three-dimensional unsteady flow past a 5:1 rectangular cylinder. Journal Wind Eng. Ind. Aerodyn, 99, 469–482.
- S. M. Fraser and C. Carey, 1990. Numerical and experimental analysis of flow around isolated and shielded cubes. Appl. Math. Modelling, 14, 588-597.
- Bosch G. and Rodi W., 1998. Simulation of vortex shedding past a square cylinder with different turbulence models. International Journal for Numerical Methods in Fluids. 28, 601–616.
- Kimura I. and Hosoda T., 2003. A non-linear k-ε model with realizability for prediction of flows around bluff bodies. International Journal for Numerical methods in fluids. 42, 813–837.
- Shilpa G., Harikrishna p., Santhi A.S., Ramesh Babu G., 2014. Evaluation of Aerodynamic Pressure and Force coefficients for a 1:2:5Rectangular Building Model under Uniform Flow Condition in Wind Tunnel. Proceedings of the International Conference on Advances in Sustainability of Materials and Environment, Nagercoil. 10-11, 72-82.
- IS: 875 (Part3)-1987.Code of practice for design loads (other than earthquake) for buildings and structures.

**BIOGRAPHIES**

**G Naga Sulochana** received his B.Tech in civil engineering from AVR & SVR COLLEGE OF ENGINEERING AND TECHNOLOGY, NANDYAL. Under JNTU ANATAPUUR and pursuing his M.Tech in AVR & SVR COLLEGE OF ENGINEERING AND TECHNOLOGY, NANDYAL.



**H Sarath kumar** received his M.Tech in structural Engineering from Annamarachaya College Of Engineering Tirupathi,. And working as Assistant Professor with 1-years of experience as a Assistant Professor in AVR & SVR COLLEGE OF ENGINEERING AND TECHNOLOGY, NANDYAL